Effect of Narrow-Band Frequency Modulated Force on Horseshoe Chaos in Double-Well Duffing-vander Pol Oscillator

L.Ravisankar, V.Ravichandran, V.Chinnathambi, S.Rajasekar

Abstract— This paper investigates both analytically and numerically the effect of narrow-band frequency modulated (NBFM) force on horseshoe chaos in double-well Duffing-vander Pol (DVP) oscillator. Using Melnikov method an analytical threshold condition for the prediction of onset of horseshoe chaos is obtained. Melnikov threshold curves are drawn in different external parameters space. Parametric regimes where suppression of horseshoe chaos occurs are predicted. Analytical predictions are demonstrated through direct numerical simulations. Starting from asymptotic chaos we show the recovery of periodic motions for a range of values of amplitude and frequency of the external force. Interestingly suppression of chaos is found in the parametric regimes where the Melnikov function does not change sign. Various routes to chaos and crisis are found to occur due to the NBFM force. Numerical investigations including computation of stable and unstable manifolds of saddle, Maximal Lyapunov exponent, Poincarè map and bifurcation diagram are used to detect horseshoe chaos.

Keywords— Chaos, Controlling chaos, Duffing-vander Pol oscillator, Horseshoe chaos, Homoclinic bifurcation, Narrow-band frequency modulated force, Melnikov method,

1 INTRODUCTION

Over the past years the study of effect of different periodic forces on nonlinear systems has received much attention. The study of effect of such periodic forces will be helpful to choose a suitable external drive in creating and controlling nonlinear behaviours. In recent years there are reports on the effect of different forces on certain nonlinear phenomenon [1], [2], [3], [4], [5], [6], [7], [8], [9], [10]. It is also important to explore the utility and applicability of analytical methods such as multiple-scale perturbation method and Melnikov method to the system driven by periodic forces other than $f\sin\omega t$ or $f\cos\omega t$.

L.Ravisankar is currently working as Assistant Professor of Physics, Sri K.G.S. Arts College, Srivaikuntam-628 619, Tamilnadu,India.
V.Ravichandran is currently working as Associate Professor of Physics, Sri K.G.S. Arts College, Srivaikuntam-628 619, Tamilnadu, India.
V.Chinnathambi is currently working as Associate Professor of Physics, Sri K.G.S. Arts College, Srivaikuntam-628619, Tamilnadu ,India. Email: veerchinnathambi@gmail.com
S.Rajasekar is working as Professor in School of Physics, Bharadidasan University, Tiruchirapalli-620 024, Tamilnadu, India.

Melnikov technique [11], [12] is one of the few analytical methods available for determining the existence of chaotic motion in near-integrable systems subject to dissipative time-dependent perturbation. The main idea of Melnikov technique is to find a function that can measure the distance between stable and unstable manifolds for a saddle of a perturbed system. If the function vanishes for a certain bifurcation parameter value, then stable and unstable manifolds will intersect each other away from the saddle points or points in the Poincarè section and thus forming a type of Smale's horseshoe mapping leading to chaos. Recently, this method has been applied to certain nonlinear systems [6], [7], [13], [14], [15], [16], [17], [18], [19], [20]

In this paper we investigate analytically and numerically, the effect of Narrow-Band Frequency Modulated (NBFM) force in double-well Duffing-van der Pol oscillator equation

$$\ddot{x}+\rho\dot{x}(1-x^2)-\alpha^2x+\beta x^3=f(\cos\omega t-g\sin\Omega t\sin\omega t), \quad (1)$$

where f is the unmodulated carrier amplitude, g is the modulation index, ω and Ω are the two frequencies of the external force. The motivation for our interest in this system is that it has wide range of applications in physics and biology. It describes the dynamics of charged

density in plasma of a rf gas discharge. It exhibits well developed chaos in the parameter space [21], [22], [23], [24]. The parametrically driven case of (1) in the absence of external forcing $f = 0, g = 0$ was studied numerically by Zielinska et al. [25] who found that the system exhibits chaotic behavior. Recently, Balachandran et al. [26] designed and investigated a new higher order autonomous vander Pol-Duffing oscillator based on fifth order hyperchaotic circuit to improve secure communication. Lai et al. [27] investigated the possibility of suppression of jamming and stochastic resonance by both narrow-band and wide-band frequency modulated signals in FitzHugh-Nagumo oscillator and Lorenz equations. Our objective is to study the effect of NBFM force on horseshoe chaos using both numerical and analytical techniques. In our present analysis we use Melnikov analytical method to study the influence of NBFM force on homodinic orbits.

The remainder of the present paper proceeds as follows. In the next section we discuss the application of the Melnikov method and obtain the Melnikov function for the system (1). The external force has two frequencies ω and Ω. In section 3 we consider the case of $\omega=\Omega$ and derive the threshold condition on the parameters f and g for the transverse intersection of homoclinic orbits. Then we plot the Melnikov threshold curve with $g=0$ and $g\neq 0$ in the parameter spaces (f,ω) and $(g,\Omega(=\omega))$. The analytical predictions are demonstrated through direct numerical simulations. Starting from horseshoe chaos we show the possibility of its suppression. The case of $\omega \neq \Omega$ is also discussed at the end of this section. In section 4 we analyze numerically the periodic and chaotic behaviours of the system (1). We show the examples of period-doubling, intermittency and quasiperiodic routes to chaos for some specific sets of values of the parameters. Finally, section 5 contains conclusion.

2 Melnikov analysis

We are considering here the perturbed DVP oscillator (1) with the NBFM force , which is given by

$$\dot{x} = y, \qquad (2a)$$

$$\dot{y} = \alpha^2 x - \beta x^3 - \in[p(1-x^2)y + f(\cos\omega t - g\sin\Omega t \sin\omega t)], \qquad (2b)$$

where $\in$ is a small parameter, $\alpha^2>0$ and $\beta > 0$. We next derive the fixed points and the phase portrait corresponding to the unperturbed system. If we let $\in=0$, the unperturbed system can be written as

$$\dot{x} = y, \qquad \dot{y} = \alpha^2 x - \beta x^3, \qquad (3)$$

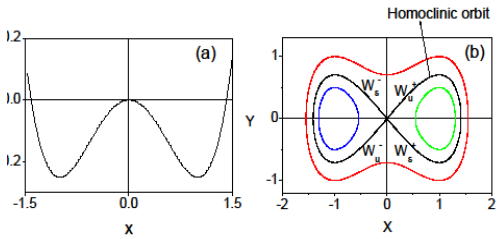

Figure 1. (a) The two-well potential function for the unperturbed system (3). (b) Phase trajectories of the unperturbed system (3). The stable $(W_s^{\pm})$ and unstable $(W_u^{\pm})$ parts of homoclinic orbits connecting saddle to itself are indicated. The analytical expression for the homoclinic orbits is given by (6).

which corresponds to an integrable Hamiltonian system with the potential function given by

$$V(x) = -\frac{1}{2}\alpha^2 x^2 + \frac{1}{4}\beta x^4. \qquad (4)$$

Shape of the potential function is shown in Fig. 1(a) and whose associated Hamiltonian function is

$$H(x,y) = \frac{1}{2}y^2 - \frac{1}{2}\alpha^2 x^2 + \frac{1}{4}\beta x^4. \qquad (5)$$

By analyzing the unperturbed system, we can observe that there are three different equilibria one saddle fixed point $(x^*, y^*) = (0,0)$ and two centre type fixed points $(\pm\alpha/\sqrt{\beta}, 0)$. The two homoclinic orbits which connect saddle to itself are given by

$$W^{\pm}(x_h(\tau), y_h(\tau)) = \pm\alpha\sqrt{2/\beta}\,\mathrm{sech}(\alpha\tau), \mp\alpha^2\sqrt{2/\beta}\,\mathrm{sech}(\alpha\tau)\tanh(\alpha\tau) \quad . \qquad (6)$$

where $\tau = t - t_0$. Stable manifolds $(W_s^{\pm})$ and unstable manifolds $(W_u^{\pm})$ of homoclinic orbits are indicated in Fig. 1(b). Periodic orbits are nested within and outside the homoclinic orbits. For $\in=0$, the stable and unstable branches of homoclinic orbits join smoothly. When the dissipative perturbation is included the stable manifold W_s and the unstable manifold W_u do not join. However, above

certain critical amplitude and frequency of the external periodic force, transverse intersections of W_s and W_u occur. In order to apply the Melnikov method, in general, we rewrite the given equation of motion into the following standard form

$$\dot{x} = f_1(x,y) + \in g_1(x,y,t), \tag{7a}$$

$$\dot{y} = f_2(x,y) + \in g_2(x,y,t). \tag{7b}$$

where g_1 and g_2 are periodic in t with period T. Further the unperturbed system [$\in = 0$ in (7)] should possess atleast one hyperbolic fixed point and an integrable separatrix solution passing through the point. For the standard form of the (7), the Melnikov integral is

$$M(t_0) = \int_{-\infty}^{\infty} [f_1 g_2 - f_2 g_1] \exp\left[-\int_0^t \left[\left(\frac{\partial f}{\partial x}\right) - \left(\frac{\partial f}{\partial y}\right) \right] dt' \right] d\tau. \tag{8}$$

For the DVP (2) the Melnikov integral (8) works out to be

$$M^{\pm}(t_0) = A \pm B f \sin\omega t_0 \pm C g \sin(\omega + \Omega) t_0 \mp D g \sin(\omega - \Omega) t_0, \tag{9a}$$

where

$$A = \frac{4}{3}\frac{p\alpha^3}{\beta}\left[1 - \frac{4\alpha^2}{5\beta}\right], \tag{9b}$$

$$B = \sqrt{2/\beta}\,\pi\omega \sec h(\pi\omega/2\alpha), \tag{9c}$$

$$C = \sqrt{2/\beta}\,\pi(\omega+\Omega) \sec h(\pi(\omega+\Omega)/2\alpha), \tag{9d}$$

$$D = \sqrt{2/\beta}\,\pi(\omega-\Omega) \sec h(\pi(\omega-\Omega)/2\alpha). \tag{9e}$$

From the above relations we can obtain the condition for transverse intersection of stable manifolds $W_S^{\pm}$ and unstable manifolds ($W_U^{\pm}$) that is $M^{\pm}(t_0)$ to change sign at some t_0.

3 Analytical and Numerical results

In this section, we analyze the effect of NBFM with the frequency $\omega = \Omega$ and $\omega \neq \Omega$.

3.1 Effect of NBFM force with $\omega = \Omega$

We analyze the occurrence of homoclinic bifurcation and onset of chaos for three different cases separately, such as (i) $g = 0$ and f is varied, (ii) g fixed and f varied and (iii) f fixed and g varied. For $g=0$ the system is driven by the sinusoidal force $f\cos\omega t$ and Melnikov function becomes

$$M^{\pm}(t_0) = A \pm B f \sin\omega t_0. \tag{10}$$

From the above relation we can obtain the threshold curve for getting horseshoe chaos in the parameter space (p, α, β, f). For example, fixing $p, \alpha, \beta,$ we have the following threshold curve in the (ω, f) plane

$$|f| \geq |f_M| = \frac{2\sqrt{2}p\alpha^3\left[1 - \frac{4\alpha^2}{5\beta}\right]}{3\sqrt{\beta}\,\pi\omega} \cosh\ \pi\omega/2\alpha\ . \tag{11}$$

Equation (11) is the necessary condition for the existence of horseshoe chaos. The sufficient condition requires the existence of simple zeros of $M(t_0)$. When (11) becomes an equality, the zero of M is nontransverse and this corresponds to tangential intersection where $dM/dt = 0$ at $t = t_0$.

In Fig. 2, we have plotted f as a function of the frequency ω for $\alpha = 1.0, \beta = 5.0, p = 0.4$ and $g=0$. In the parameter region, below the threshold curve no transverse intersection of stable and unstable manifolds of the saddle occurs and above the threshold curve transverse intersections of stable and unstable manifolds of the saddle occur. Just above the Melnikov threshold curve onset of cross well chaos is expected. We have verified the above analytical prediction by direct numerical simulation of the system (1). As an example Fig. 3 shows the numerically computed W_s and W_u of the saddle in Poincarè map for $f = 0.075$ and $f = 0.2$ with ω=1.0. The unstable manifolds are obtained by integrating (1) in

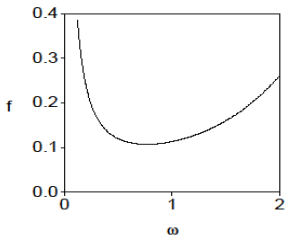

Figure 2. Threshold curve for horseshoe chaos in the (f, ω) plane for $\alpha = 1.0, \beta = 5.0, p = 0.4$ and $g=0$. Above the curve transverse intersections of homoclinic orbits occur.

the forward time for a set of 900 initial conditions chosen around the perturbed saddle point. The saddle manifolds are obtained by integrating the (1) in reverse time. For f= **0.075** the two orbits are well separated for which the Melnikov distance is always positive (Fig. 3(a)). For $f = 0.2$, (Fig. 3(b)) we can clearly notice transverse intersection of the two orbits where the Melnikov distance oscillates between positive and negative values. For ω=1, analytically predicted Melnikov threshold value is $f_M = 0.1132$. The corresponding numerical value is found to be $f_N = 0.125$, which is greater than f_M value as expected. For $f < 0.125$ asymptotically periodic motion is observed. Onset of chaotic motion is observed at $f = 0.125$ at which the Melnikov distance becomes zero for some $t=t_0$. Thus for $f \geq 0.125$ it is possible to have either asymptotic chaos or transient chaos followed by asymptotically periodic motions.

Now we consider the effect of NBFM force for the second case, that is, by fixing the value of g and thereby varying f. For $\omega=\Omega$, we have D=0 in (9(e)) and the Melnikov function is given by (9(a)) becomes

$$M^{\pm}(t_0) = A \pm Bf \sin\omega t_0 \pm Cg \sin 2\omega t_0. \qquad (12)$$

The necessary condition on f for $M(t_0)$ to change sign is

$$f \geq f_M^{\pm} = (A \pm Cg)/B, \qquad (13a)$$

(*or*)

$$f \leq f'^{\pm}_M = (-A \pm Cg)/B. \qquad (13b)$$

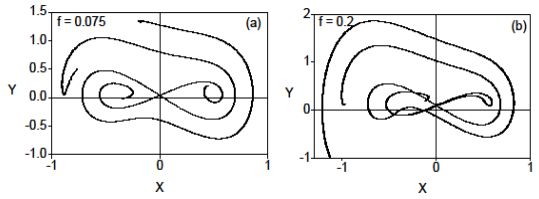

Figure 3. Numerically computed stable and unstable manifolds of saddle for the DVP oscillator (Eq.1) in the x, y plane for f = 0.075 and 0.2. The values of the other parameters are $\alpha = 1.0, \beta = 5.0, p = 0.4, \omega = 1.0$ and g=0.

where the superscript signs '+' and '−' corresponds to the homoclinic orbits W^+ and W^- respectively. In general, for arbitrary values of ω and Ω, the above condition is not sufficient to ensure the existence of simple zeros of $M(t_0)$ in (9). However the condition (13) is sufficient if the frequency Ω, is in resonance with ω, that is $v\Omega = u\omega$ $(\Omega/\omega = u/v)$ where v and u are some positive integers.

Fig. 4 shows the Melnikov threshold curves for horseshoe chaos in (f, Ω) plane for $\omega = \Omega, \alpha = 1.0, \beta = 5.0, p = 0.4$ and g=0.1. In the (f, Ω) parameter space transverse intersections of both orbits, that is W_s^+ and W_u^+ and W_s^- and W_u^- occur in the regions a and e. That is in these regions both $M^+(t_0)$ and $M^-(t_0)$ to change sign.

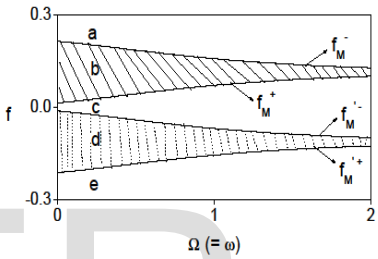

Figure 4. Melnikov threshold curves for horseshoe chaos in (f, Ω) plane for $\alpha = 1.0, \beta = 5.0, p = 0.4, \omega = 1.0$ and g=0.1.

While one can expect transverse intersections of W_s^+ and W_u^+ in the region b. This implies that in this region $M^+(t_0)$ alone changes sign and the sign of $M^-(t_0)$ remains same. In the region d transverse intersection W_s^- and W_u^- alone occur since in this region only $M^-(t_0)$ changes sign. Thus horseshoe chaos occur in the entire (f, Ω) parameter space. However in the region c, only $M^+(t_0)$ and $M^-(t_0)$ do not change sign and is an indication of no tranverse intersection of orbits of saddle. For $\omega = \Omega = 1$, when the forcing amplitude f is increased from a value in the region e of both orbits occur for $f > f_M^- = 0.156$. The above analytical transverse intersection of stable and unstable parts of W^+ and W^- occur for $f < f'^+_M = -0.156$; intersection of stable and unstable manifolds of W^- alone occur for $f'^+_M = -0.156 < f < f'^-_M = -0.07$; no transverse intersection of manifolds of W^- and W^+ occur for $f'^-_M = -0.07 < f < f_M^+ = +0.07$; transverse intersection of

manifolds of W^+ alone occur for $f_M^+ = 0.07 < f < f_M^- = 0.156$ and transverse intersection of both orbits occur for $f > f^-_M = 0.156$. The above analytical

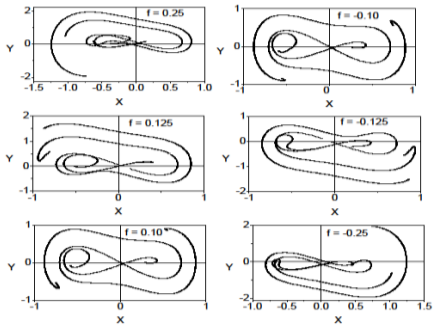

Figure 5. Numerically computed stable and unstable manifolds of saddle for six values of **f**. The values of the other parameters are fixed at $\alpha = 1.0, \beta = 5.0, p = 0.4, \omega = \Omega$ and g=0.1.

results are verified by direct numerical simulations of DVP (1). As an example, in Fig. 5, we have shown the stable and unstable orbits of saddle in the Poincarè map for six values of f chosen in the regions a, b, c, d and e with $\omega = \Omega = 1$ and g=0.1. Transverse intersections of stable and unstable branches of both the homoclinic orbits occur for $f = \pm 0.25$ which fall in the regions a and e. For $f = \pm 0.125$ (corresponding to regions b and d) we see transverse intersection of homoclinic orbits at only one point. When $f = \pm 0.10$ (in region c) no transverse intersection of the orbits occur. The stable and unstable

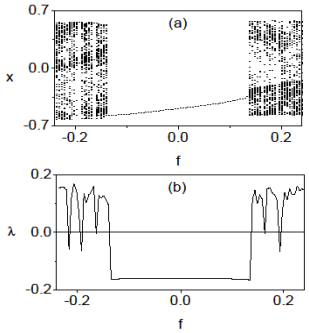

Figure 6. Bifurcation diagram and the corresponding maximal Lyapunov exponent diagram for the DVP oscillator driven by the NBFM force with $\omega = \Omega = 1.0$ and g=0.1.

Orbits are well separated. These numerical results agree well with the theoretical predictions.

In order to know the nature of attractors of the system near the horseshoe threshold curve, we have further numerically investigated the (1) and the onset of chaos therein. Fig. 6(a) shows the bifurcation diagram where we have plotted x *vs* f for every period of the external force after omitting the initial transient evolution. The maximal Lyapunov

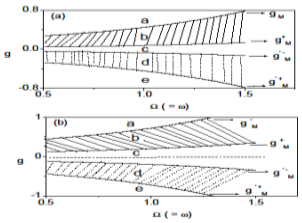

Figure 7. Melnikov threshold curves for horseshoe chaos in (g, Ω) plane for (a) $f = 0.08$ and (b) $f = 0.2$. The values of the other parameters are $\alpha = 1.0, \beta = 5.0, p = 0.4$ and $\omega = \Omega$. The dashed curve represents transverse intersections of orbits of saddle.

exponent (λ) is computed using the algorithm given in the ref. [28] and is reported in Fig. 6(b). In the regions b and d of Fig. 4 where intersections of the orbits of W^- and intersections of the orbits of W^+ alone occur, respectively, the long time evolution is found to be periodic. From the bifurcation diagram the onset of chaos are found to occur at $f = \pm 0.1379$, whereas the Melnikov threshold values for transverse intersection of stable and unstable branches of the both homoclinic orbits are ± 0.131. The analytical prediction is in good agreement with the actual numerical analysis of the system.

Then we consider the effect of NBFM force for the third case, that is, by fixing the value of f and thereby varying g. For a fixed value of f, the necessary condition on g for $M(t_0)$ to change sign is

$$g \geq g_M^{\pm} = (A \pm Bf)/C, \qquad (14a)$$

(*or*)

$$g \leq g'^{\pm}_M = (-A \pm Bf)/C. \qquad (14b)$$

Fig. (7) shows the Melnikov threshold curves for horseshoe chaos in the (g, Ω) plane for $f = 0.08$ and $f = 0.2$ with $\Omega = \omega$. The values of the other parameters are $\alpha = 1.0, \beta = 5.0$ and $p = 0.4$. When g=0 and $f = 0.08$ as shown in Figs. 2 and 3 no transverse intersection of homoclinic orbits occurs. However as g is varied from

zero, above certain critical value horseshoe chaos occurs. In the regions a and e both $M^+(t_0)$ and $M^-(t_0)$ change sign and the transverse intersections of stable and unstable parts of W^+ and W^- occur. Transverse intersections of W_s^+ and W_u^+ alone happen in the region b. In the region c, no transverse intersections of both stable and unstable manifolds of saddle occur. In the region d transverse

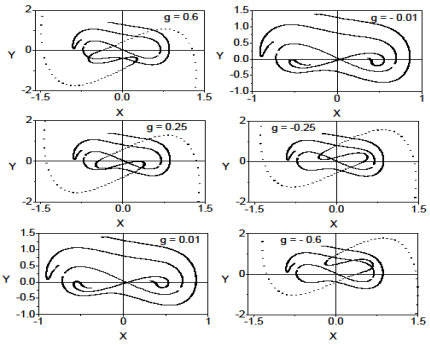

Figure 8. Numerically computed stable and unstable manifolds of saddle for $\alpha = 1.0, \beta = 5.0, p = 0.4, \omega = \Omega = 1.0$ and $f = 0.08$.

intersections of W_u^- and W_s^- alone take place. The above analytical results are also verified by direct simulation of the system (1). Fig. 8 shows the part of stable and unstable orbits in the Poincarè map for the six values of g chosen in the regions a, b, c, d and e with $\omega = \Omega = 1$ and $f = 0.08$. Transverse intersections of both the homodinic orbits occur for g=0.6 which is above the threshold value $g_M^- = 0.402$. This value of g falls in the region a. For $f = 0.25$ (corersponding to the region b) we notice the tranverse intersections of W_s^- and W_u^- alone at two places. When g=±0.01 (in the region c) no transverse intersections of orbits occur. For g=-0.25 as expected we see only the transverse intersection of W_s^+ and W_u^+. Intersections of both the homoclinic orbits are clearly seen for g=-0.6 which falls in the region e. When g=0, the Melnikov threshold values for transverse intersection are $f_M^{\pm} = \pm 0.1132$. We fix f at 0.2 above the threshold value 0.1132 and study the effect of the modulating term by varying g. Fig. 7(b) shows the Melnikov threshold curves for transverse intersections of homoclinic orbits. For $f = 0.2$ and g=0 transverse intersections of stable and unstable manifolds of saddle This is Melnikov threshold occur for a range of values of ω (see Fig. 3). curves for transverse intersections of homoclinic orbits. For $f = 0.2$ and g=0 transverse intersections of stable and unstable manifolds of saddle occur for a range of values of ω (see Fig. 3). This is represented by the dashed line in Fig. 7(b). When g is switched on, even for small values of g, the transverse intersections suddenly disappear. That is, horseshoe chaos is suppressed. This occurs for a range of values of g. In region c, no transverse intersection of homoclinic orbits occur. In regions b and d tranverse intersections of W^+ and W^- take place. In the regions a and e intersections of both the homoclinic orbits occurs.

Finally, we consider the effect of NBFM force for the case of $\Omega \neq \omega$ that is $\Omega/\omega \neq u/v$. In general for arbitrary values of ω and Ω, conditions similar to Eqs. (13) or (14) cannot be written to ensure the existence of simple zeros of $M(t_0)$ in (9(a)). However, the occurrence of horseshoe chaos can be studied numerically by measuring the time τ_M elapsed between two successive transverse intersections. τ_M can be determined from (9). In Fig. 9 we have plotted $1/\tau_M^{\pm}$ as a function of Ω, for $\omega = 1.0, \alpha = 1.0, \beta = 5.0, p = 0.4, f = 0.08$ and g=0.1. Continuous curve corresponds to positive sign while dashed curve corresponds to negative sign in (9). Horseshoe chaos does not occur when $1/\tau_M$ is zero and it occurs in the region where $1/\tau_M > 0$. In Fig. 9, for $f = 0.08$, both $1/\tau_M^+$ and $1/\tau_M^-$ are zero. (that is $\tau_M^{\pm}$ is infinity) at $\Omega = 0.875, 0.95$ and 1.0. This implies that horseshoe chaos does not occur for $\Omega = 0.875, 0.95$ and 1.0. For other values of Ω, both

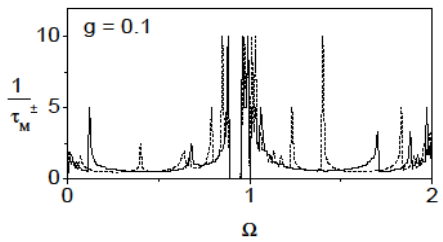

Figure 9. Variation of $1/\tau_M^{\pm}$ versus Ω, for $\omega = 1.0$ and $f = 0.08$. Continuous curve is for positive sign and dashed curve is for negative sign of $M(t_0)$ given by Eq. (9).

$M^{+}(t_0)$ and $M^{-}(t_0)$ oscillate and hence $1/\tau_M^{+}$ are non zero. These results are verified numerically.

4 Numerical predictions of periodic and chaotic behaviours of the system (1)

In this section for some specific sets of values of control parameters we show the occurrence of period doubling, intermittency and quasiperiodic routes to chaos and suppression of chaos in the presence of NBFM force.

We fix the values of the parameters as $\alpha = 1.0, \beta = 5.0, p = 0.4$ and $\omega = \Omega = 1.0$. Fig. 10(a) shows the bifurcation diagram drawn between x *vs* f and g is set to zero. As f is increased from zero, the period-1 solution exists in the range $0 < f < 0.108695$ and then it loses its stability at the critical values of $f = f_1 = 0.108695$ giving birth to (or bifurcating into) a period-2T orbit. System-1 then undergoes further period-doubling bifurcations as the control parameter f is smoothly varied. For example, period-2 orbit exists in the range $0.108695 < f < 0.109483$ and it becomes unstable at $f = 0.109483$ giving birth to a period-4T orbit. This cascade of bifurcation continues further as 8T, 16T… orbits and accumulates at $f = f_C = 0.110047$. At this critical value of f onset of chaotic motion occurs. When the parameter f is further increased from f_C, the dynamics of the interval $0.110047 < f < 0.25$ is more complicated and intricate. This interval of f is not fully occupied by chaotic takes place at different critical values of f. Particularly the asymptotic motion consists of chaotic orbits interspersed by periodic orbits (windows), period-doubling windows, band–merging and sudden-widening chaotic attractors and intermittency route to chaos. For clarity, band- merging, orbits alone, but many fascinating changes in the dynamics sudden-widening bifurcations and intermittency route to chaos are shown in Fig. 11. At $f = 0.25$, chaotic motion suddenly disappears and the long time motion settles to a periodic behavior. The influence of the control parameter f on the dynamics for the two fixed values of g namely $g=0.1$ (periodic region) and 0.3 (chaotic region) is also studied. The effect of f can be clearly seen in the bifurcation diagrams Figs. 10(b) and 10(c). Here again suppression of chaos is found for certain range of values of the control parameter f.

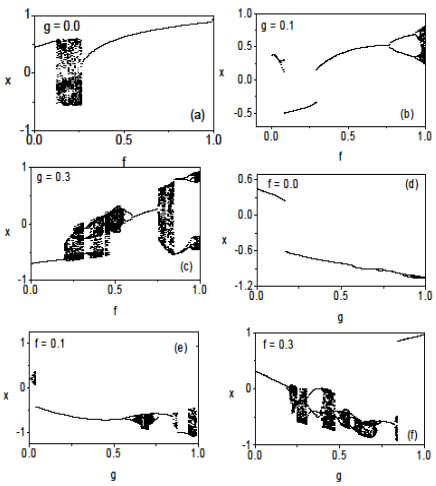

Fig.10. Bifurcation structures for the system (1) for $\alpha = 1.0, \beta = 5.0, p = 0.4, \omega = \Omega = 1.0$.

Next we show the effect of the control parameter g by fixing the value of f. Fig. 10(d) shows the bifurcation diagram obtained by varying g from 0 to 1 where f is set to zero. The long-time motion settles to a periodic behavior and chaotic motion appears in a small region. The effect of g can be clearly seen in the bifurcation diagrams Fig. 10(e)

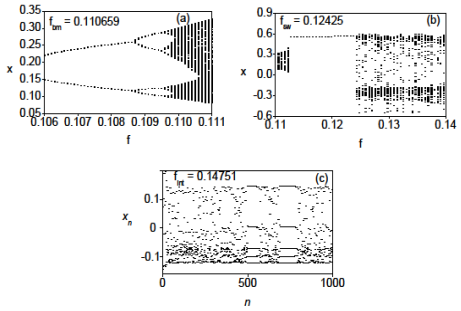

Figure 11. (a) Band-merging (b) sudden-widening and (c) intermittency route to chaos. The values of the other parameters are $\alpha = 1.0, \beta = 5.0, p = 0.4, g = 0.0, \omega = \Omega = 1.0$.

and 10(f) for another two fixed values of f that is, $f = 0.1$ (lies in the periodic region) and 0.3 (lies in the chaotic region). Here again suppression of chaos is found for certain range of values of the control parameter g.

5 Conclusion

In the present paper we have studied the effect of NBFM force on horseshoe chaos and routes to asymptotic chaos in a linearly damped Duffing-vander Pol oscillator both analytically and numerically. Using Melnikov analytical method we obtained the threshold condition for onset of horseshoe chaos that is transverse intersection of stable and unstable branches of homoclinic orbits. Threshold curves are drawn in different parameters space. We have verified the analytical predictions through numerical simulation. Near the Melnikov threshold curve, onset of chaos is observed. We discussed the effect of other parameters such as f, g and Ω, on the dynamics of the system (1). It is important to study the effect of wide-band frequency modulated force on horseshoe and asymptotic chaos in DVP oscillator. This will be investigated in future.

REFERENCES

[1] R.Chacon, "Control of Homoclinic Chaos by Weak Periodic Perturbations," *World Scientific*, Singapore, 2005.
[2] K.Konishi, "Generating Chaotic Behaviours in an Oscillator Driven by Periodic Forces, " *Phys. Lett. A*, 2003; 320: 200-206.
[3] Z.M.Ge and W.Y.Leu, "Anticontrol of Chaos of Two Degrees of Freedom Loud Speaker System and Synchronization of Different Order Systems," *Chaos, Solitons & Fractals*, 2004; 20: 503-521.
[4] V.M.Gandhimathi, K.Murali and S.Rajasekar, "Stochastic Resonance with Different Periodic Forces in Overdamped Two Coupled Anharmonic Oscillators," *Chaos, Solitons & Fractals*, 2006; 30: 1034-1047.
[5] V.M.Gandhimathi, S.Rajasekar and J.Kurths , "Effects of the Shape of Periodic Forces on Stochastic Resonance," *Int. J. of Bifur. & Chaos*, 2008; 18: 2073- 2088.
[6] V.Ravichandran, V.Chinnathambi and S.Rajasekar, "Effect of Rectified and Modulated Sine Forces on Chaos in Duffing Oscillator," *Indian J. of Physics*, 2009; 83: 1593-1603.
[7] V.Ravichandran, V.Chinnathambi and S.Rajasekar, "Homoclinic Bifurcation and Chaos in Duffing Oscillator Driven by Amplitude Modulated Force," *Physica A*, 2007; 376: 223- 236.
[8] V.Ravichandran, V.Chinnathambi and S.Rajasekar, "Study of Nonescape Dynamics in Duffing Oscillator with Four Different Periodic Forces ," Indian J. of *Physics*, 2012; 86: 907- 911.
[9] A.Venkatesan , S.Parthasarathy and M.Lakshmanan, "Occurrence of Multiple Period-Doubling Bifurcation Route to Chaos in Periodically Pulsed Chaotic Dynamical Systems," *Chaos, Solitons and Fractals*, 2003; 18: 891- 898.
[10] R.Chacon, "Inhibition of Chaos in Hamiltonian Systems by Periodic Pulse," *Phys. Rev. E*, 1994; 50: 750-753.
[11] J.Guckenheimer and P.J.Holmes, "Nonlinear Oscillations, Dynamical Systems and Bifurcations of Vector Fields," Springer, New York, 1983.
[12] S.Wiggins, "Introduction to Applied Nonlinear Dynamical Systems and Chaos," Springer, New York, 1990.
[13] H.Cao and G.Chen, "Global and Local Control of Homoclinic and Heteroclinic Bifurcation," *Int. J. Bifur. Chaos*, 2005; 15: 2411-2432.
[14] H.Cao, "Primary Resonant Optimal Control for Homoclinic Bifurcation in Single-Degree of Freedom Nonlinear Oscillators," *Chaos, Solitons & Fractals*, 2005; 24: 1387-1398.
[15] S.Rajasekar, "Controlling of Chaos by Weak Periodic Perturbations in DVP Oscillator," *Pramana J. of Physics*, 1993; 41: 295-309.
[16] Z.H.Liu and W.Q.Zhu, "Homoclinic Bifurcation and Chaos in Simple Pendulum under Bounded Noise Excitations," *Chaos, Solitons & Fractals*, 2004; 20: 593-607.
[17] M.Siewe Siewe, H.Cao and M.A.F.Sanjuan," On the Occurrence of Chaos in a Parametrically Driven Extended Rayleigh Oscillator with Three-Well Potential," *Chaos, Solitons & Fractals*, 2009; 41: 772-782.
[18] M.Borowiec, G.Litak and A.Syta, "Vibration of the Duffing Oscillator: Effect of Fractional Damping'', *Shock and Vibration*, 2007; 14: 29-36.
[19] P.Zhou and H.Cao, "The Effect of Symmetry-Breaking on the Parametrically Excited Pendulum," *Chaos, Solitons & Fractals*, 2008; 38: 590-597.
[20] K.I.Thomas and G.Ambika, "Suppression of Smale Horseshoe Structure via Secondary Perturbation in Pendulum Systems," *Pramana J. of Physics*, 1999; 52: 375-387.
[21] J.Fang, "Generalized Farey Organization and Generalized Winding Number in a 2-D DDDS," *Phys. Lett. A*, 1990; 146: 35-44.
[22] S.Rajasekar, S.Parthasarathy and M.Lakshmanan, "Predictions of Horseshoe Chaos in BVP and DVP Oscillators," *Chaos, Solitons and Fractals*, 1992; 2: 271-280.
[23] G.P.King and S.T.Gaito, "Bistable Chaos I. Unfolding the Cusp," *Phys. Rev. A*, 1992; 46: 3092-3099.
[24] M.G.M.Gomes and G.P.King, "Bistable Chaos II. Bifurcation Analysis," *Phys. Rev. A*, 1992; 46: 3100- 3110.
[25] B.J.A.Zielinska, D.Mukamel, V.Steinberg and S.Fishman, "Chaotic Behaviour in Externally Modulated Hydrodynamic System," *Phy. Rev. A*, 1985; 32: 702-704.
[26] V.Balachandran and G.Kandiban, "Experimental and Numerical Realization of Higher Order Autonomous Van der Pol-Duffing Oscillator, "*Indian J. of Pure and Applied Physics*, 2009; 47: 823-827.
[27] Y.C.Lai, Z.Liu, A.Nachman and L.Zhu, " Suppression of Jamming in Excitable Systems by Aperiodic Stochastic Resonance," *Int. J. Bifur. & Chaos*, 2004; 14: 3519-3539 .
[28] A.Wolf, J.B.Swift, H.L.Swinny and J.A.Vastano, "Determining Lyapunov Exponents From a Time Series," *Physica D*, 1985; 16: 285-317.